

# Isospin breaking in the pion–nucleon scattering lengths

Martin Hoferichter<sup>a</sup>, Bastian Kubis<sup>a</sup>, Ulf-G. Meißner<sup>a,b</sup>

<sup>a</sup>Helmholtz–Institut für Strahlen- und Kernphysik (Theorie) and Bethe Center for Theoretical Physics, Universität Bonn, D-53115 Bonn, Germany

<sup>b</sup>Institut für Kernphysik (Theorie), Institute for Advanced Simulations, and Jülich Center for Hadron Physics, Forschungszentrum Jülich, D-52425 Jülich, Germany

## Abstract

We analyze isospin breaking through quark mass differences and virtual photons in the pion–nucleon scattering lengths in all physical channels in the framework of covariant baryon chiral perturbation theory.

**Key words:** Pion–baryon interactions, Chiral Lagrangians, Electromagnetic corrections to strong-interaction processes

**PACS:** 13.75.Gx, 12.39.Fe, 13.40.Ks

## 1. Introduction

Isospin violation in the Standard Model is driven by strong and electromagnetic interactions, that is by the differences in the light quark masses and charges, respectively. As already stressed by Weinberg, the pion–nucleon scattering lengths offer a particularly good testing ground for strong isospin violation [1]. This problem was addressed in the framework of heavy-baryon chiral perturbation theory (ChPT) in a series of papers about a decade ago [2, 3, 4, 5, 6]. Recently, new interest arose in high-precision calculations of the pion–nucleon scattering lengths. First, the accurate measurements of the characteristics of pionic hydrogen and deuterium allow one in principle to extract certain  $\pi N$  scattering lengths to high precision. This, however, is only possible if isospin breaking is taken into account consistently. In the case of the strong energy shift of the ground state of pionic hydrogen one needs the isospin-violating contributions to  $a_{\pi^- p \rightarrow \pi^- p}$ . In [7], these have been determined at third order in the chiral expansion,  $\mathcal{O}(p^3)$ , in a covariantly regularized form of baryon ChPT [8]. [For a recent review on baryon ChPT, see [9].] As for the width of pionic hydrogen, the knowledge of the isospin-breaking corrections to  $a_{\pi^- p \rightarrow \pi^0 n}$  is required. In the analysis of pionic deuterium isospin violation is particularly important, since the  $\pi d$  scattering length at leading order is proportional to the small isoscalar scattering length  $a^+$  and therefore chirally suppressed (cf. [10]). Since  $\text{Re } a_{\pi d} \propto a_{\pi^- p \rightarrow \pi^- p} + a_{\pi^- n \rightarrow \pi^- n} + \text{few-body corrections}$ , we may improve at least the two-body contributions by extending the isospin-breaking corrections to  $a_{\pi^- n \rightarrow \pi^- n}$  to  $\mathcal{O}(p^3)$ . Second, as has been stressed in particular by Bernstein, threshold pion photoproduction offers the unique possibility of measuring the so far undetermined  $\pi^0 p$  scattering length and gives access to the charge exchange scattering length  $a_{\pi^+ n \rightarrow \pi^0 p}$ , see [11] and the recent review [12]. Such measurements are becoming feasible at HIγS and at MAMI. In view of these developments, it is timely to extend the work of [7] to *all* charge channels in pion–nucleon scattering.

## 2. Formalism

We start the description of various formal aspects of  $\pi N$  scattering at threshold with the kinematics. The momenta of the nucleon and pion in the initial (final) state will be denoted by  $p$  ( $p'$ ) and  $q$  ( $q'$ ), respectively, their masses by  $m_i$  ( $m_f$ ) and  $M_i$  ( $M_f$ ).  $m_p$ ,  $m_n$ ,  $M_\pi$ , and  $M_{\pi^0}$ , are the masses of proton, neutron, and charged and neutral pion. We define the isospin limit by the charged particle masses  $m_p$  and  $M_\pi$ . Working at first order in isospin breaking, i.e. at  $\mathcal{O}(e^2, m_d - m_u) \equiv \mathcal{O}(\delta)$ , we only need contributions linear in  $\Delta_\pi = M_\pi^2 - M_{\pi^0}^2$  and  $\Delta_N = m_n - m_p$ .

For elastic scattering, the kinematics at threshold are determined by

$$s = (m_i + M_i)^2, \quad p = p' = \frac{m_i}{M_i} q = \frac{m_i}{M_i} q', \quad t = 0. \quad (1)$$

(1) is modified for the charge exchange reactions (cex) according to

$$p \neq p', \quad q \neq q', \quad t = -\Delta_\pi + \frac{M_\pi}{m_i + M_\pi} (m_f^2 - m_i^2 + \Delta_\pi). \quad (2)$$

In loop contributions that only start at  $\mathcal{O}(p^3)$ , these kinematical relations may be chirally expanded, leading to

$$s = (m_p + M_\pi)^2, \quad t = -\Delta_\pi, \quad p = p' = \frac{m_p}{M_\pi} q. \quad (3)$$

Note that still  $q'$  must not be replaced by  $q$ , since the difference is of the same chiral order as  $q$  and  $q'$  themselves.

The pion–nucleon scattering amplitude  $T_{\pi N}$  is parameterized in terms of the two amplitudes  $D(s, t)$  and  $B(s, t)$  according to

$$T_{\pi N} = \bar{u}(p') \left( D(s, t) - \frac{1}{2(m_i + m_f)} [q', q] B(s, t) \right) u(p),$$

$$\bar{u}(p') u(p') = 2m_f, \quad \bar{u}(p) u(p) = 2m_i. \quad (4)$$

In the isospin limit,  $T_{\pi N}$  may be decomposed as

$$T^{ab} = T^+ \delta^{ab} + T^- \frac{1}{2} [\tau^a, \tau^b], \quad (5)$$

where  $a$  ( $b$ ) is the isospin index of the outgoing (incoming) pion and  $\tau^i$  are the Pauli-matrices. Using the Condon–Shortley phase convention, the physical amplitudes are related to  $T^+$  and  $T^-$  by

$$\begin{aligned} T_{\pi^- p} &\equiv T_{\pi^- p \rightarrow \pi^- p} = T_{\pi^+ n} \equiv T_{\pi^+ n \rightarrow \pi^+ n} = T^+ + T^-, \\ T_{\pi^+ p} &\equiv T_{\pi^+ p \rightarrow \pi^+ p} = T_{\pi^- n} \equiv T_{\pi^- n \rightarrow \pi^- n} = T^+ - T^-, \\ T_{\pi^- p}^{\text{cex}} &\equiv T_{\pi^- p \rightarrow \pi^0 n} = T_{\pi^+ n}^{\text{cex}} \equiv T_{\pi^+ n \rightarrow \pi^0 p} = -\sqrt{2} T^-, \\ T_{\pi^0 p} &\equiv T_{\pi^0 p \rightarrow \pi^0 p} = T_{\pi^0 n} \equiv T_{\pi^0 n \rightarrow \pi^0 n} = T^+. \end{aligned} \quad (6)$$

For the elastic channels only  $D(s, t)$  contributes at threshold, whereas we find for the charge exchange reactions

$$T_{\pi N} = 2\sqrt{m_n m_p} \left( \left( 1 + \frac{\Delta_\pi}{8m_p^2} \right) D_{\text{thr}} - \frac{M_\pi \Delta_\pi}{4m_p^2} B_{\text{thr}} \right), \quad (7)$$

where  $D_{\text{thr}}$  and  $B_{\text{thr}}$  denote the amplitudes evaluated at threshold. The correction factor in front of  $D$  stems from the expansion of the Dirac spinors around the isospin limit. Since the prefactor is already of first order in  $\delta$ ,  $B_{\text{thr}}$  may be evaluated assuming isospin symmetry to relate it to isovector threshold parameters [13],

$$\begin{aligned} B_{\text{thr}}^- &= 8\pi m_p \left( \frac{a_{0+}^-}{4m_p^2} + a_{1-}^- - a_{1+}^- \right) \\ &= \frac{1}{2F_\pi^2} (1 + 4m_p c_4) + \mathcal{O}(p), \quad B_{\text{thr}} = -\sqrt{2} B_{\text{thr}}^-, \end{aligned} \quad (8)$$

where  $a_{l\pm}^-$  denotes the isovector scattering lengths with orbital momentum  $l$  and total angular momentum  $l \pm \frac{1}{2}$ . For brevity, we will use  $a^\pm \equiv a_{0\pm}^\pm$  for the S-wave isoscalar and isovector scattering lengths. Equation (8) also shows the leading chiral representation of  $B_{\text{thr}}^-$ . All relevant terms of the effective chiral Lagrangians defining the corresponding low-energy constants are collected in Appendix A.

The S-wave scattering length  $a$  for elastic scattering of scalar particles is related to the amplitude  $T(s, t)$  by

$$a = \frac{1}{8\pi\sqrt{s}} T(s, t) \Big|_{|\mathbf{p}| \rightarrow 0}, \quad (9)$$

where  $|\mathbf{p}|$  is the center-of-mass momentum. This result is generalized to pion–nucleon scattering by

$$\begin{aligned} a_{\text{elastic}} &= \frac{m_i}{4\pi(m_i + M_i)} D_{\text{thr}}^{\text{elastic}}, \\ a_{\text{cex}} &= \frac{\sqrt{m_p m_n}}{4\pi(m_i + M_\pi)} \left\{ \left( 1 + \frac{\Delta_\pi}{8m_p^2} \right) D_{\text{thr}}^{\text{cex}} - \frac{M_\pi \Delta_\pi}{4m_p^2} B_{\text{thr}}^{\text{cex}} \right\}. \end{aligned} \quad (10)$$

The isospin-symmetric contributions to the scattering lengths have already been worked out in [14]. Adapted to our notation they read

$$\begin{aligned} a^+ &= \frac{m_p M_\pi^2}{4\pi(m_p + M_\pi) F_\pi^2} \left\{ -\frac{g_A^2}{4m_p} + 2(c_2 + c_3 - 2c_1) + \frac{3g_A^2 M_\pi}{64\pi F_\pi^2} \right\}, \\ a^- &= \frac{m_p M_\pi}{8\pi(m_p + M_\pi) F_\pi^2} \left\{ 1 + \frac{g_A^2 M_\pi^2}{4m_p^2} + \frac{M_\pi^2}{8\pi^2 F_\pi^2} \left( 1 - \log \frac{M_\pi^2}{\mu^2} \right) \right. \\ &\quad \left. + 8M_\pi^2 (d_1^\pi + d_2^\pi + d_3^\pi + 2d_5^\pi) + \frac{2M_\pi^2}{F_\pi^2} l_4^\pi \right\}. \end{aligned} \quad (11)$$

As soon as we take into account virtual photons, we have to specify more carefully what we mean by  $D_{\text{thr}}$  due to the appearance of threshold divergences. First of all, we subtract all one-photon-reducible diagrams, since they diverge  $\sim 1/t$ , and denote the result by  $\tilde{D}$ . The additional divergences due to photon loops may be regularized in the form

$$\left( e^{iQ\alpha\theta_C(|\mathbf{p}|)} \tilde{D}(s, t) \right) \Big|_{|\mathbf{p}| \rightarrow 0} = \frac{\beta_1}{|\mathbf{p}|} + \beta_2 \log \frac{|\mathbf{p}|}{\mu_c} + D_{\text{thr}} + \mathcal{O}(|\mathbf{p}|), \quad (12)$$

where  $\alpha = e^2/4\pi$  denotes the fine structure constant,  $\theta_C(|\mathbf{p}|)$  the infrared divergent Coulomb phase given by

$$\theta_C(|\mathbf{p}|) = -\frac{\mu_c}{|\mathbf{p}|} \log \frac{m_\gamma}{2|\mathbf{p}|}, \quad (13)$$

and  $\mu_c = m_p M_\pi / (m_p + M_\pi)$  the reduced mass of the incoming particles.  $Q$  accounts for the charges of the particles involved, explicitly

$$Q_{\pi^- p} = -2, \quad Q_{\pi^+ p} = 2, \quad Q_{\pi^- p}^{\text{cex}} = -1, \quad (14)$$

and  $Q = 0$  for the remaining channels. For consistency reasons, the contribution from  $B(s, t)$  to the charge exchange reaction should be multiplied by the same phase as  $\tilde{D}(s, t)$ . Since  $\alpha\theta_C(|\mathbf{p}|)$  is of first order in isospin breaking, this does not lead to additional terms at the order considered here, but makes it obvious that  $\theta_C(|\mathbf{p}|)$  drops out of physical observables. The coefficients  $\beta_i$  may be related to the scattering lengths  $a$ . The explicit relation

$$\beta_1 = -\frac{\pi}{2} Q e^2 M_\pi a \quad (15)$$

is confirmed by our calculation at leading order in the chiral expansion, but can be proven to hold in general in the framework of non-relativistic effective field theories [15, 16]. The coefficient  $\beta_2$  only appears at two-loop level.

### 3. Analytic results

The topologies of the Feynman diagrams contributing at threshold are displayed in Fig. 1. There are significantly less diagrams than above threshold, since many diagrams which are formally of  $\mathcal{O}(p^3)$  start only at  $\mathcal{O}(p^4)$  for the following reasons. Firstly, the leading term of a particular diagram can be determined by simplifying the numerators according to chiral power counting, making use of (1) and (3). With  $\Sigma = p + q$  and loop momentum  $k$  a typical example for such a simplification is

$$\begin{aligned} (\not{\Sigma} - \not{k} + m_p) \not{q} \gamma_5 (\not{p} - \not{k} + m_p) &\rightarrow (\not{p} + m_p) \frac{M_\pi}{m_p} \not{p} \gamma_5 (\not{p} + m_p) \\ &= -\gamma_5 \frac{M_\pi}{m_p} \not{p} (-\not{p} + m_p) (\not{p} + m_p) = 0. \end{aligned} \quad (16)$$

Secondly, all  $s$ -channel one-particle-reducible diagrams involve structures of the type  $(\not{\Sigma} + m_p) \not{q} \gamma_5 u(p)$ , whose leading part vanishes at threshold, since

$$\begin{aligned} (\not{\Sigma} + m_p) \not{q} \gamma_5 u(p) &\rightarrow (\not{p} + m_p) \frac{M_\pi}{m_p} \not{p} \gamma_5 u(p) \\ &= \frac{M_\pi}{m_p} \not{p} \gamma_5 (-\not{p} + m_p) u(p) = 0. \end{aligned} \quad (17)$$

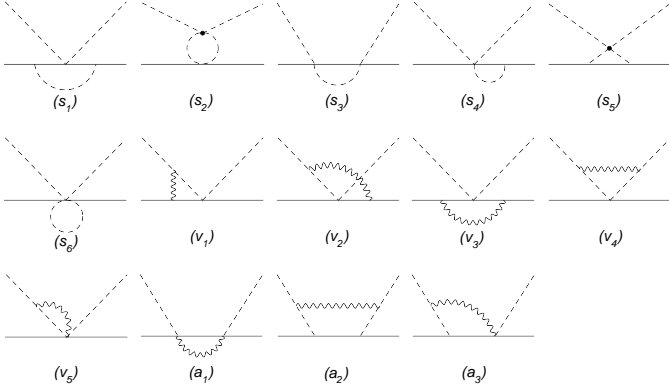


Figure 1: Loop diagrams for  $\pi N$  scattering at threshold. Solid, dashed, and wiggly lines, denote nucleons, pions, and photons, respectively. Crossed diagrams and diagrams contributing via wave function renormalization only are not shown.

The  $u$ -channel diagrams are treated analogously. Unfortunately, both arguments only work for  $q$  and not for  $q'$  in the charge exchange reactions, unless the diagram in question is already of order  $\mathcal{O}(\delta)$ ; but eventually one can show that all diagrams which may be omitted in the case of the elastic channels do not contribute to the charge exchange reactions either.

Concentrating on the analysis of the isospin-breaking shifts in the scattering lengths, we obtain the following results for the reaction channels on the proton (the neutron channels can be found in Appendix B):

$$\begin{aligned}
\Delta a_{\pi^- p} &= a_{\pi^- p} - (a^+ + a^-) = \Delta a^+ + \Delta a^- + i \text{Im} a_{\pi^- p}, \\
\Delta a_{\pi^+ p} &= a_{\pi^+ p} - (a^+ - a^-) = \Delta a^+ - \Delta a^-, \\
\Delta a^+ &= \frac{m_p}{4\pi(m_p + M_\pi)} \left\{ \frac{4\Delta_\pi}{F_\pi^2} c_1 - \frac{e^2}{2} (4f_1 + f_2) \right. \\
&\quad \left. - \frac{g_A^2 M_\pi}{32\pi F_\pi^2} \left( \frac{33\Delta_\pi}{4F_\pi^2} + e^2 \right) \right\} \\
\Delta a^- &= -\frac{m_p M_\pi}{4\pi(m_p + M_\pi)} \left\{ \frac{\Delta_\pi}{32\pi^2 F_\pi^4} \left( 3 + \log \frac{M_\pi^2}{\mu^2} \right) \right. \\
&\quad + \frac{8\Delta_\pi}{F_\pi^2} d_5^r + \frac{e^2 g_A^2}{16\pi^2 F_\pi^2} \left( 1 + 4 \log 2 + 3 \log \frac{M_\pi^2}{\mu^2} \right) \\
&\quad \left. - 2e^2 \left( g_6^r + g_8^r - \frac{5}{9F_\pi^2} (k_1^r + k_2^r) \right) \right\}, \\
\text{Im} a_{\pi^- p} &= \frac{m_p}{4\pi(m_p + M_\pi)} \left\{ \frac{M_\pi^2}{8\pi F_\pi^4} \sqrt{\Delta_\pi - 2M_\pi \Delta_N} + \frac{e^2 g_A^2 M_\pi}{4\pi F_\pi^2} \right\}, \\
\Delta a_{\pi^- p}^{\text{cex}} &= a_{\pi^- p}^{\text{cex}} + \sqrt{2} a^- = \frac{\sqrt{2} m_p}{4\pi(m_p + M_\pi)} \left\{ \frac{e^2 f_2}{2} \right. \\
&\quad + \frac{g_A^2 \Delta_\pi}{4F_\pi^2 m_p} + \frac{M_\pi \Delta_\pi}{4m_p^2} \left( B_{\text{thr}}^- - \frac{3}{4F_\pi^2} \right) + \frac{8M_\pi \Delta_\pi}{F_\pi^2} d_5^r \\
&\quad + \frac{M_\pi \Delta_\pi}{192\pi^2 F_\pi^4} \left( 2 - 7g_A^2 + (2 - 5g_A^2) \log \frac{M_\pi^2}{\mu^2} \right) \\
&\quad \left. + \frac{e^2 M_\pi}{32\pi^2 F_\pi^2} \left( 5 + 3 \log \frac{M_\pi^2}{\mu^2} \right) - \frac{M_\pi \Delta_N}{4F_\pi^2 m_p} (1 + 2g_A^2) \right\}
\end{aligned}$$

$$+ \frac{e^2 M_\pi}{2F_\pi^2} \left( F_\pi^2 g_7^r - 2k_3^r + k_4^r + \frac{20}{9} (k_1^r + k_2^r) \right) \Bigg\},$$

$$\begin{aligned}
\Delta a_{\pi^0 p} &= a_{\pi^0 p} - a^+ = -\frac{\Delta_\pi}{M_\pi^2} a^+ + \frac{m_p}{4\pi(m_p + M_\pi)} \left\{ \frac{3g_A^2 M_\pi \Delta_\pi}{128\pi F_\pi^4} \right. \\
&\quad \left. - \frac{M_\pi^2 \sqrt{\Delta_\pi + 2M_\pi \Delta_N}}{8\pi F_\pi^4} + \frac{2c_5 B(m_d - m_u)}{F_\pi^2} \right\}. \quad (18)
\end{aligned}$$

We wish to point explicitly to the square-root-like terms in  $\text{Im} a_{\pi^- p}$  and  $\Delta a_{\pi^0 p}$ , which are caused by the unitarity cusps due to the different thresholds of the  $\pi^0 n$  and  $\pi^+ n$  intermediate states, respectively. These cusps can be calculated exactly at threshold, which we will illustrate for the imaginary part in Sect. 4.3. Since the cusp is of order  $\mathcal{O}(\sqrt{\delta})$  and thus enhanced compared to the other isospin-breaking effects, we also take into account the correction by  $\Delta_N$ , although this is formally an  $\mathcal{O}(p^4)$  effect. Nevertheless, it contributes  $\sim 30\%$  to the difference between  $a_{\pi^0 p}$  and  $a_{\pi^0 n}$  (see Appendix B).

We have performed the following checks on our calculation: the amplitudes are ultraviolet-finite, all ultraviolet divergences due to loops are canceled by the infinite parts of the counterterms (as calculated in [7]). Thus, only the renormalized counterterms appear in (18). They compensate the scale dependence generated by the chiral logarithms, such that the final results are independent of the renormalization scale  $\mu$ . Furthermore, the infrared divergences caused by virtual photons cancel among themselves, as they should.

A useful way to quantify isospin-breaking corrections in terms of measurable quantities is the so-called triangle relation that vanishes in the isospin limit. It is defined as

$$R = 2 \frac{a_{\pi^+ p} - a_{\pi^- p} - \sqrt{2} a_{\pi^- p}^{\text{cex}}}{a_{\pi^+ p} - a_{\pi^- p} + \sqrt{2} a_{\pi^- p}^{\text{cex}}}, \quad (19)$$

where only the real parts of the scattering lengths are inserted. At first order in  $\delta$  we obtain

$$\begin{aligned}
R &= \frac{m_p}{4\pi(m_p + M_\pi) a^-} \left\{ \frac{e^2 f_2}{2} + \frac{g_A^2 \Delta_\pi}{4F_\pi^2 m_p} - \frac{M_\pi \Delta_N}{4F_\pi^2 m_p} (1 + 2g_A^2) \right. \\
&\quad - \frac{3M_\pi \Delta_\pi}{16F_\pi^2 m_p^2} + \frac{M_\pi \Delta_\pi}{4m_p^2} B_{\text{thr}}^- - \frac{M_\pi \Delta_\pi}{48\pi^2 F_\pi^4} \left( 4 + \log \frac{M_\pi^2}{\mu^2} \right) \\
&\quad - \frac{g_A^2 M_\pi \Delta_\pi}{192\pi^2 F_\pi^4} \left( 7 + 5 \log \frac{M_\pi^2}{\mu^2} \right) + \frac{e^2 M_\pi}{32\pi^2 F_\pi^2} \left( 5 + 3 \log \frac{M_\pi^2}{\mu^2} \right) \\
&\quad - \frac{e^2 g_A^2 M_\pi}{16\pi^2 F_\pi^2} \left( 1 + 4 \log 2 + 3 \log \frac{M_\pi^2}{\mu^2} \right) \\
&\quad \left. + \frac{e^2 M_\pi}{2} (4g_6^r + g_7^r + 4g_8^r) + \frac{e^2 M_\pi}{2F_\pi^2} (k_4^r - 2k_3^r) \right\}. \quad (20)
\end{aligned}$$

We refrain from constructing an isoscalar triangle relation from the three elastic pion-proton scattering lengths (cf.  $R_1$  in [3]); such a relation can easily be read off from the results in (18). It depends on the low-energy constants  $f_1$ ,  $f_2$ , and  $c_1$ , and, as we will see in the following section, therefore cannot be very well constrained, such that no additional information beyond the shifts in the individual scattering lengths is provided.

## 4. Numerical results

### 4.1. Low-energy constants

The most precise values for  $a^+$  and  $a^-$  stem from an analysis of pionic hydrogen and pionic deuterium data [10]

$$a^+ = (1.5 \pm 2.2) \cdot 10^{-3} M_\pi^{-1}, \quad a^- = (85.2 \pm 1.8) \cdot 10^{-3} M_\pi^{-1}. \quad (21)$$

In addition, the authors extract the electromagnetic low-energy constant (LEC)  $f_1 = -2.1_{-2.2}^{+3.2} \text{ GeV}^{-1}$ .  $f_2$  and  $c_5$  can be deduced from the mass difference between proton and neutron. This mass difference comprises electromagnetic as well as strong contributions

$$m_n - m_p = -4Bc_5(m_d - m_u) + f_2 e^2 F_\pi^2, \quad (22)$$

which may be disentangled by means of the Cottingham formula [17]. The result of this procedure is  $f_2 = -(0.97 \pm 0.38) \text{ GeV}^{-1}$ ,  $Bc_5(m_d - m_u) = -(0.51 \pm 0.08) \text{ MeV}$ .

In [18], various previous analyses of  $c_1$  are briefly reviewed and combined to  $c_1 = -0.9_{-0.5}^{+0.2} \text{ GeV}^{-1}$ . For  $d_5^r$ , we will use  $F_\pi^2 d_5^r(\mu) = (0.6 \pm 3.0) \cdot 10^{-3}$ , specifying the renormalization scale to  $\mu = 1 \text{ GeV}$ . The central value is the mean of the values quoted in [13] (translated to our conventions regarding  $\mathcal{L}_\pi^{(p^4)}$ ), where a low-energy theorem linking  $d_5^r$  to a certain subthreshold parameter of  $\pi N$  scattering is derived. In the spirit of the treatment of  $c_1$ , we estimate the error by investigating the effects of higher orders in this low-energy theorem. Neglecting the fourth order contribution would shift  $F_\pi^2 d_5^r$  by

$$\frac{M_\pi}{16} \frac{64m_p c_1 + g_A^2 [2(4 + g_A^2) + \sqrt{2} \log(1 + \sqrt{2})]}{32\pi m_p} = -3 \cdot 10^{-3} \quad (23)$$

(for the central value of  $c_1$ ). The resulting uncertainty ensures consistency with most values for  $d_5^r$  available in the literature [6, 19, 20, 21, 22, 23].

We now turn to the determination of  $B_{\text{thr}}^-$ . Values for  $a_{1-}^-$  and  $a_{1+}^-$  can be found in [21, 22, 23, 24]. Using

$$a_{1-}^- = (-12 \pm 2) \cdot 10^{-3} M_\pi^{-3}, \quad a_{1+}^- = (-81 \pm 6) \cdot 10^{-3} M_\pi^{-3} \quad (24)$$

yields

$$B_{\text{thr}}^- = (0.60 \pm 0.06) \cdot 10^{-3} \text{ MeV}^{-2}. \quad (25)$$

Since the main source for the determination of  $c_4$  are  $\pi N$  threshold data, it seems more reliable to apply the threshold parameters directly.

Estimates of the meson-sector electromagnetic LECs  $k_i$  are given in [25] using resonance saturation [26, 27]. Unfortunately, this method does not provide reliable error estimates. The central values for the  $k_i$  in question are  $k_1^r = 10.9 \cdot 10^{-3}$ ,  $k_2^r = 0.7 \cdot 10^{-3}$ ,  $k_3^r = 3.9 \cdot 10^{-3}$ ,  $k_4^r = -1.3 \cdot 10^{-3}$  (all at  $\mu = 1 \text{ GeV}$ ). Since  $g_6^r$ ,  $g_7^r$ , and  $g_8^r$  are not known, they are set to zero in the numerical work. Particle masses and decay constants are taken from [28], in particular  $F_\pi = 92.2 \text{ MeV}$  and  $|g_A| = 1.2695$ .

### 4.2. Triangle relation, scattering lengths

The triangle relation  $R$  can be determined rather well since  $f_1$ , the  $\mathcal{O}(p^2)$  LEC which is least known, drops out. The central value is obtained by inserting the above LECs and (21) into (20). As for the error, we are faced with the following combination of electromagnetic LECs whose uncertainty is not known:

$$k_4^r - 2k_3^r + F_\pi^2(4g_6^r + g_7^r + 4g_8^r). \quad (26)$$

Naively one would assign the order-of-magnitude errors  $1/16\pi^2$  to each LEC and add the individual contributions in quadrature. However, this may underestimate the uncertainty in case the variation of the renormalization scale  $\mu$  by a factor of  $e = 2.718 \dots$ , controlled by the corresponding  $\beta$ -functions, induces a change significantly larger than  $1/16\pi^2$ . Assuming  $1 \text{ GeV}$  to be a ‘‘natural’’ scale for hadronic processes, this running covers the energy range the physics we consider should be sensitive to. Estimating the uncertainty by varying the LECs according to their  $\beta$ -functions in a correlated way has the further advantage of being independent under redefinition of the Lagrangian. The result of this procedure is

$$R = (1.5 \pm 0.2 f_2 \pm 0.03 a^- \pm 0.03 B_{\text{thr}}^- \pm 1.1_{\text{LEC}}) \% \\ = (1.5 \pm 1.1) \%, \quad (27)$$

where the different contributions to the error are denoted by a subscript, ‘‘LEC’’ standing here and in the following for the corresponding combination of LECs with unknown error. The final uncertainty is obtained by adding the individual contributions in quadrature. Naive order-of-magnitude arguments would reduce the error significantly to  $0.4 \%$ . The large error in (27) is dominated by the  $g_i^r$ , as may be seen from their  $\beta$ -functions [7]  $\eta_7 = -9/2 - 2Z(5g_A^2 + 1)/3 = -9.4$ ,  $\eta_8 = -2\eta_6 = 3(4g_A^2 - 1)/2 + 2Z(5g_A^2 + 1)/3 = 13.1$ , which are by no means of order  $\mathcal{O}(1)$ .

We now turn to the isospin-violating contributions to the individual scattering lengths. The procedure as described above yields

$$\Delta a_{\pi^- p} = \left( -3.4_{-2.9}^{+1.2} c_1 - 5.7_{f_1}^{+3.9} \pm 0.2 f_2 \pm 0.6 d_5 \pm 1.2_{\text{LEC}} + 5.0i \right) 10^{-3} M_\pi^{-1} \\ = \left( -3.4_{-6.5}^{+4.3} + 5.0i \right) \cdot 10^{-3} M_\pi^{-1}, \\ \Delta a_{\pi^+ p} = \left( -5.3_{-2.9}^{+1.2} c_1 - 5.7_{f_1}^{+3.9} \pm 0.2 f_2 \pm 0.6 d_5 \pm 1.2_{\text{LEC}} \right) \cdot 10^{-3} M_\pi^{-1} \\ = -5.3_{-6.5}^{+4.3} \cdot 10^{-3} M_\pi^{-1}, \\ \Delta a_{\pi^- p}^{\text{cex}} = \left( 0.4 \pm 0.2 f_2 \pm 0.8 d_5 \pm 0.04 B_{\text{thr}}^- \pm 0.4_{\text{LEC}} \right) \cdot 10^{-3} M_\pi^{-1} \\ = (0.4 \pm 0.9) \cdot 10^{-3} M_\pi^{-1}, \\ \Delta a_{\pi^0 p} = \left( -5.2 \pm 0.1 a^+ \pm 0.2 c_5 \right) \cdot 10^{-3} M_\pi^{-1} \\ = (-5.2 \pm 0.2) \cdot 10^{-3} M_\pi^{-1}. \quad (28)$$

Discarding the imaginary part, (28) corresponds to relative changes compared to the isospin limit of  $-3.9_{-7.5}^{+4.9} \%$  in  $a_{\pi^- p}$ ,  $+6.4_{-5.1}^{+7.8} \%$  in  $a_{\pi^+ p}$ , and  $(-0.4 \pm 0.8) \%$  in  $a_{\pi^- p}^{\text{cex}}$ . Due to the poor knowledge of  $a^+$ , the corresponding normalization of  $\Delta a_{\pi^0 p}$  is not very meaningful; note that the isospin-breaking shift  $\Delta a_{\pi^0 p}$  in (28) is significantly larger than  $a^+$ . As already pointed out

in [7], the large isospin-breaking corrections to the charged-pion elastic channels can be traced back to the triangle graph ( $s_5$ ) (see Fig. 1), which however only yields a rather small contribution to the charge exchange reaction. In contrast, isospin violation in the neutral-pion elastic channel is predominantly due to the cusp effect enhanced by  $\sqrt{\delta}$ . The large uncertainties in  $\Delta a_{\pi^\pm p}$  are dominated by  $f_1$  and  $c_1$  that are part of  $\Delta a^+$  in (18), therefore appear in the same combination with  $a^+$  in both channels.

### 4.3. Imaginary parts

Exact expressions for the imaginary parts of  $a_{\pi^- p}$  and  $a_{\pi^- p}^{\text{cex}}$  generated by the  $\pi^0 n$  and  $\gamma n$  intermediate states can be obtained using Cutkosky rules, expressing the vertices at threshold by scattering lengths and electric dipole amplitudes  $E_{0+}$  encountered in the context of pion photoproduction. Retaining all chiral orders, the resulting imaginary parts up to  $\mathcal{O}(\delta)$  are

$$\text{Im} \begin{Bmatrix} a_{\pi^- p} \\ a_{\pi^- p}^{\text{cex}} \end{Bmatrix} = \frac{a^- \sqrt{2m_p}}{\sqrt{m_p + M_\pi}} \sqrt{\Delta_\pi - 2M_\pi \Delta_N} \begin{Bmatrix} \sqrt{2} a^- \\ -a^+ \end{Bmatrix} + \frac{M_\pi E_{0+}(\pi^- p)}{(m_p + M_\pi)} (M_\pi + 2m_p) \begin{Bmatrix} E_{0+}(\pi^- p) \\ E_{0+}(\pi^0 n) \end{Bmatrix}. \quad (29)$$

The experimental value for  $E_{0+}(\pi^- p)$  taken from [29] and the leading term of its chiral expansion calculated in [30] up to  $\mathcal{O}(ep^3)$  are

$$E_{0+}(\pi^- p) = -\frac{\sqrt{2} eg_A}{8\pi F_\pi} + \mathcal{O}(ep) = (-31.5 \pm 0.8) \cdot 10^{-3} M_\pi^{-1}, \quad (30)$$

whereas  $E_{0+}(\pi^0 n)$  only starts at  $\mathcal{O}(ep^2)$  (explicit expressions are given in [31]); therefore both contributions to  $\text{Im} a_{\pi^- p}^{\text{cex}}$  in (29) are suppressed by at least one chiral order. Unfortunately,  $E_{0+}(\pi^0 n)$  is not directly accessible in experiment. Combining deuterium data with ChPT predictions [32] yields

$$E_{0+}(\pi^0 n) = (2.1 \pm 0.5) \cdot 10^{-3} M_\pi^{-1}. \quad (31)$$

Inserting the chiral expansions of  $E_{0+}(\pi^- p)$  and  $a^-$  into (29) reproduces the imaginary part of  $a_{\pi^- p}$  appearing in (18). One can easily check that the difference between (29) and its chiral expansion is mainly due to  $\Delta_N$ , which justifies our treatment of the cusp effect in Sect. 3. Separating strong (first number) and electromagnetic contributions, we obtain numerically

$$\begin{aligned} \text{Im} a_{\pi^- p} &= \left( (2.91 \pm 0.12) + (1.86 \pm 0.09) \right) \cdot 10^{-3} M_\pi^{-1} \\ &= (4.77 \pm 0.15) \cdot 10^{-3} M_\pi^{-1}, \\ \text{Im} a_{\pi^- p}^{\text{cex}} &= \left( (-0.04 \pm 0.05) + (-0.12 \pm 0.03) \right) \cdot 10^{-3} M_\pi^{-1} \\ &= (-0.16 \pm 0.06) \cdot 10^{-3} M_\pi^{-1}. \end{aligned} \quad (32)$$

Finally, the above results may be checked based on the observation that the ratio

$$\frac{\text{Im} a_{\pi^- p} \Big|_{\text{strong}}}{\text{Im} a_{\pi^- p} \Big|_{\text{EM}}} = 1.57 \pm 0.10 \quad (33)$$

should correspond to the so-called Panofsky ratio  $P = \sigma(\pi^- p \rightarrow \pi^0 n) / \sigma(\pi^- p \rightarrow \gamma n)$ . Indeed, its experimental value is found to be  $P = 1.546 \pm 0.009$  (cf. [33, 34]).

## 5. Comparison to earlier work

Our result for  $\pi^- p \rightarrow \pi^- p$  agrees with [7]. In [3], a similar analysis of isospin breaking was performed in heavy-baryon ChPT, switching off virtual photons. This corresponds to

$$\Delta_\pi \neq 0, \Delta_N \neq 0, f_1 e^2 \neq 0, f_2 e^2 \neq 0, m_d \neq m_u, e^2 = 0. \quad (34)$$

Furthermore, isospin-breaking effects due to the Dirac spinors are neglected and  $B_{\text{thr}}^-$  is expressed by  $c_4$ . We have checked explicitly for the triangle relation, for the charge exchange reactions, and for the neutral-pion elastic channels, that our results coincide in this limit. Numerically, we find  $R = (0.74 \pm 0.21) \%$ , which is compatible with the numerical value  $R_{\text{FMS}} = (0.9 \dots 1.1) \%$  quoted in [3]. Both values slightly differ, since the denominator is not expressed by  $a^-$  (the additional LECs needed are taken from [21]) and since the isospin limit is defined as the average between charged and neutral particles.

Virtual photons were taken into account in [6] in order to study isospin violation above threshold. Unfortunately, a direct comparison is not possible, as no analytic expressions for the amplitudes are provided. Even more, also a numerical comparison is difficult due to a conceptual difference: in [6], the electromagnetic corrections were used to pin down the LECs from experimental data, and thereafter applied to extract the strong amplitude. In particular, electromagnetic contributions to the particle masses were switched off. Thus, the quoted isospin-breaking effect of  $-0.7 \%$  for the triangle relation in the S-wave refers to strong isospin violation only.

## 6. Summary and outlook

In this letter, we have systematically analyzed isospin violation in the  $\pi N$  scattering lengths in all channels, including a detailed estimate of the theoretical uncertainties. The extension of this analysis beyond threshold will be the subject of future work, to which we also refer for details of the calculation [35].

We find that isospin violation is quite small in  $\pi^- p \rightarrow \pi^0 n$ , at the order of one percent at most, whereas the charged-pion elastic channels display more sizeable effects on the few-percent level. In particular, the so-called triangle relation that vanishes in the isospin limit is violated by about 1.5% consistent with earlier findings in heavy-baryon ChPT and inconsistent with the 5–7% deviation extracted from the data at lowest pion momenta in [36, 37]. In addition, we find a substantial isospin-breaking correction to the neutral-pion–proton scattering length. In view of these results, further experiments e.g. at HIγS and MAMI are urgently called for.

## Acknowledgements

Partial financial support by the Helmholtz Association through funds provided to the virtual institute ‘‘Spin and strong QCD’’ (VH-VI-231), by the European Community–Research Infrastructure Integrating Activity ‘‘Study of Strongly Interacting Matter’’ (acronym HadronPhysics2, Grant Agreement n. 227431) under the Seventh Framework Programme of the EU, and by DFG (SFB/TR 16, ‘‘Subnuclear Structure of Matter’’) is gratefully acknowledged.

## A. Effective Lagrangians

We will use the effective Lagrangian for nucleons, pions, and virtual photons, as constructed in [7], whereof we actually need the following terms:

$$\begin{aligned}
\mathcal{L}_{\text{eff}} &= \sum_{i=1}^2 \left( \mathcal{L}_{\pi}^{(p^{2i})} + \mathcal{L}_{\pi}^{(e^2 p^{2i-2})} \right) + \sum_{i=1}^3 \mathcal{L}_{\text{N}}^{(p^i)} + \sum_{i=0}^1 \mathcal{L}_{\text{N}}^{(e^2 p^i)} + \mathcal{L}_{\gamma}, \\
\mathcal{L}_{\pi}^{(p^2)} + \mathcal{L}_{\pi}^{(e^2)} + \mathcal{L}_{\gamma} &= \frac{F^2}{4} \langle d^{\mu} U^{\dagger} d_{\mu} U + \chi^{\dagger} U + U^{\dagger} \chi \rangle \\
&\quad + Z F^4 \langle Q U Q U^{\dagger} \rangle - \frac{1}{4} F_{\mu\nu} F^{\mu\nu} - \frac{1}{2} (\partial_{\mu} A^{\mu})^2, \\
\mathcal{L}_{\pi}^{(p^4)} &= \frac{I_4}{4} \langle d^{\mu} U^{\dagger} d_{\mu} \chi + d^{\mu} \chi^{\dagger} d_{\mu} U \rangle, \\
\mathcal{L}_{\pi}^{(e^2 p^2)} &= F^2 \left\{ \langle d^{\mu} U^{\dagger} d_{\mu} U \rangle (k_1 \langle Q^2 \rangle + k_2 \langle Q U Q U^{\dagger} \rangle) \right. \\
&\quad + k_3 \langle d^{\mu} U^{\dagger} Q U \rangle \langle d_{\mu} U^{\dagger} Q U \rangle + \langle d^{\mu} U Q U^{\dagger} \rangle \langle d_{\mu} U Q U^{\dagger} \rangle \\
&\quad \left. + k_4 \langle d^{\mu} U^{\dagger} Q U \rangle \langle d_{\mu} U Q U^{\dagger} \rangle \right\}, \\
\mathcal{L}_{\text{N}}^{(p)} &= \bar{\Psi} \{ i \not{D} - m + \frac{1}{2} g \not{\psi} \gamma_5 \} \Psi, \\
\mathcal{L}_{\text{N}}^{(p^2)} &= \bar{\Psi} \left\{ c_1 \langle \chi_{+} \rangle - \frac{c_2}{4m^2} \langle u_{\mu} u_{\nu} \rangle D^{\mu} D^{\nu} + \text{h.c.} \right. \\
&\quad \left. + \frac{c_3}{2} \langle u_{\mu} u^{\mu} \rangle + \frac{i}{4} c_4 \sigma^{\mu\nu} [u_{\mu}, u_{\nu}] + c_5 \hat{\chi}_{+} \right\} \Psi, \\
\mathcal{L}_{\text{N}}^{(e^2)} &= F^2 \bar{\Psi} \{ f_{1/3} \langle \hat{Q}_{+}^2 \mp \hat{Q}_{-}^2 \rangle + f_2 \langle Q_{+} \rangle \hat{Q}_{+} \} \Psi, \\
\mathcal{L}_{\text{N}}^{(p^3)} &= \bar{\Psi} \left\{ -\frac{d_1}{2m} [u_{\mu}, [D_{\nu}, u^{\mu}]] D^{\nu} - \frac{d_2}{2m} [u_{\mu}, [D^{\mu}, u_{\nu}]] D^{\nu} \right. \\
&\quad + \frac{d_3}{12m^3} [u_{\mu}, [D_{\nu}, u_{\lambda}]] (D^{\mu} D^{\nu} D^{\lambda} + \text{sym}) \\
&\quad \left. + \frac{i}{2m} d_5 [\chi_{-}, u_{\mu}] D^{\mu} \right\} \Psi + \text{h.c.}, \\
\mathcal{L}_{\text{N}}^{(e^2 p)} &= \frac{i F^2}{2m} \bar{\Psi} \left\{ g_6 \langle Q_{+} \rangle \langle Q_{-} u_{\mu} \rangle D^{\mu} + g_{7/8} \langle Q_{\pm} u_{\mu} \rangle Q_{\mp} D^{\mu} \right\} \Psi + \text{h.c.},
\end{aligned} \tag{35}$$

where  $\langle A \rangle$  denotes the trace of a matrix  $A$ ,  $\hat{A} = A - \langle A \rangle / 2$  its traceless part,  $\bar{\Psi}(O + \text{h.c.})\Psi \equiv \bar{\Psi} O \Psi + \text{h.c.}$  for an operator  $O$  and

$$\begin{aligned}
d_{\mu} U &= \partial_{\mu} U - i A_{\mu} [Q, U], \quad \chi = 2B \text{diag}(m_u, m_d), \quad U = u^2, \\
F_{\mu\nu} &= \partial_{\mu} A_{\nu} - \partial_{\nu} A_{\mu}, \quad Q = \frac{e}{3} \text{diag}(2, -1), \quad Q = e \text{diag}(1, 0), \\
D_{\mu} &= \partial_{\mu} + \Gamma_{\mu}, \quad \Gamma_{\mu} = \frac{1}{2} \left( u^{\dagger} (\partial_{\mu} - i Q A_{\mu}) u + u (\partial_{\mu} - i Q A_{\mu}) u^{\dagger} \right), \\
\chi_{\pm} &= u^{\dagger} \chi u^{\dagger} \pm u \chi^{\dagger} u, \quad u_{\mu} = i \left( u^{\dagger} (\partial_{\mu} - i Q A_{\mu}) u - u (\partial_{\mu} - i Q A_{\mu}) u^{\dagger} \right), \\
Q_{\pm} &= \frac{1}{2} (u Q u^{\dagger} \pm u^{\dagger} Q u), \quad [D_{\mu}, u_{\nu}] = \partial_{\mu} u_{\nu} + [\Gamma_{\mu}, u_{\nu}].
\end{aligned} \tag{36}$$

$\Psi = (p, n)^T$  contains the nucleon fields and the matrix  $U$  collects the pion fields in the usual way.  $F$  is the pion decay constant in the chiral limit and is replaced by its physical value  $F_{\pi}$  by means of

$$F_{\pi} = F \left\{ 1 + \frac{M_{\pi}^2}{F^2} \left( I_4 - \frac{1}{16\pi^2} \log \frac{M_{\pi}^2}{\mu^2} \right) \right\} + \mathcal{O}(M_{\pi}^4), \tag{37}$$

while the chiral-limit axial charge  $g$  may be identified with its physical value  $g_A$ , since axial contributions only start at  $\mathcal{O}(p^2)$  at threshold.  $m$  denotes the nucleon mass in the chiral limit.

Changing the version of  $\mathcal{L}_{\pi}^{(p^4)}$  from [38] to [39] results in a redefinition of  $d_5^r$ . This  $\tilde{d}_5^r$  is related to our  $d_5^r$  by

$$F_{\pi}^2 \tilde{d}_5^r(\mu) = F_{\pi}^2 d_5^r(\mu) + \frac{1}{8} I_4(\mu). \tag{38}$$

Note that in this convention  $I_4$  disappears in (11).

## B. Pion–neutron scattering lengths

The strong contributions to the remaining channels are determined by charge symmetry (the discrete subgroup of the general isospin transformations that only exchanges  $u \leftrightarrow d$  on the quark level), such that only the electromagnetic parts have to be calculated explicitly: the pion mass difference alone cannot contribute to charge-symmetry breaking. [How to simplify a calculation of isospin-breaking effects by such considerations is explained in more detail in [40].] The results are

$$\begin{aligned}
\Delta a_{\pi^+ n} &= a_{\pi^+ n} - (a^+ + a^-) = \left( -4.3_{-6.5}^{+4.3} + 6.0i \right) \cdot 10^{-3} M_{\pi}^{-1} \\
&= \Delta a_{\pi^- p} + \frac{e^2 m_p}{4\pi(m_p + M_{\pi})} \left\{ f_2 - 2M_{\pi} (2g_6^r + g_8^r) \right. \\
&\quad \left. + i \frac{M_{\pi}^2}{8\pi F_{\pi}^4} \left( \sqrt{\Delta_{\pi} + 2M_{\pi} \Delta_{\text{N}}} - \sqrt{\Delta_{\pi} - 2M_{\pi} \Delta_{\text{N}}} \right) \right\}, \\
\Delta a_{\pi^- n} &= a_{\pi^- n} - (a^+ - a^-) = -6.2_{-6.5}^{+4.3} \cdot 10^{-3} M_{\pi}^{-1} \\
&= \Delta a_{\pi^+ p} + \frac{e^2 m_p}{4\pi(m_p + M_{\pi})} \left\{ f_2 + 2M_{\pi} (2g_6^r + g_8^r) \right\}, \\
\Delta a_{\pi^+ n}^{\text{cex}} &= a_{\pi^+ n}^{\text{cex}} + \sqrt{2} a^- = (2.3 \pm 0.9) \cdot 10^{-3} M_{\pi}^{-1} \\
&= \Delta a_{\pi^- p}^{\text{cex}} + \frac{\sqrt{2} m_p}{4\pi(m_p + M_{\pi})} \left\{ \frac{M_{\pi} \Delta_{\text{N}}}{2F_{\pi}^2 m_p} (1 + 2g_A^2) - e^2 f_2 \right\}, \\
\Delta a_{\pi^0 n} &= a_{\pi^0 n} - a^+ = (-1.8 \pm 0.2) \cdot 10^{-3} M_{\pi}^{-1} \\
&= \Delta a_{\pi^0 p} + \frac{m_p}{4\pi(m_p + M_{\pi})} \left\{ -\frac{4c_5 B(m_d - m_u)}{F_{\pi}^2} \right. \\
&\quad \left. + \frac{M_{\pi}^2}{8\pi F_{\pi}^4} \left( \sqrt{\Delta_{\pi} + 2M_{\pi} \Delta_{\text{N}}} - \sqrt{\Delta_{\pi} - 2M_{\pi} \Delta_{\text{N}}} \right) \right\}.
\end{aligned} \tag{39}$$

$a_{\pi^+ n}^{\text{cex}}$ , which is accessible through the cusp in neutral-pion photoproduction on the proton, receives only moderate isospin-breaking corrections ( $(-1.9 \pm 0.8)\%$ ), whose uncertainty is rather well-controlled. The correction to the two-body contribution to  $\text{Re } a_{\pi d} \propto 2(a^+ + \Delta \tilde{a}^+) + \dots$  displays the same dependence on  $f_1$  and  $c_1$  as  $2(a^+ + \Delta a^+)$ . It is determined by

$$\begin{aligned}
\Delta \tilde{a}^+ &= \frac{m_p}{4\pi(m_p + M_{\pi})} \left\{ \frac{4\Delta_{\pi}}{F_{\pi}^2} c_1 - e^2 (2f_1 - M_{\pi} (2g_6^r + g_8^r)) \right. \\
&\quad \left. - \frac{g_A^2 M_{\pi}}{32\pi F_{\pi}^2} \left( \frac{33\Delta_{\pi}}{4F_{\pi}^2} + e^2 \right) \right\},
\end{aligned} \tag{40}$$

which, in addition to  $f_1$  and  $c_1$ , also includes a sizeable fixed shift (cf. the discussion in [41, 42]). Finally, we point out that the remnants of the cusp effect contribute roughly one third to the difference  $a_{\pi^0 p} - a_{\pi^0 n} = (-3.4 \pm 0.4) \cdot 10^{-3} M_{\pi}^{-1}$  and hence modify Weinberg's prediction [1] significantly. [This is in apparent contrast to the finding in [4] where the complete  $\mathcal{O}(p^4)$  corrections to  $a_{\pi^0 p} - a_{\pi^0 n}$  have been calculated; however, the result for the cusp is incorrect.]

## References

- [1] S. Weinberg, *Trans. New York Acad. Sci.* **38** (1977) 185.
- [2] U.-G. Meißner and S. Steininger, *Phys. Lett. B* **419** (1998) 403 [arXiv:hep-ph/9709453].
- [3] N. Fettes, U.-G. Meißner and S. Steininger, *Phys. Lett. B* **451** (1999) 233 [arXiv:hep-ph/9811366].
- [4] G. Müller and U.-G. Meißner, *Nucl. Phys. B* **556** (1999) 265 [arXiv:hep-ph/9903375].
- [5] N. Fettes and U.-G. Meißner, *Phys. Rev. C* **63** (2001) 045201 [arXiv:hep-ph/0008181].
- [6] N. Fettes and U.-G. Meißner, *Nucl. Phys. A* **693** (2001) 693 [arXiv:hep-ph/0101030].
- [7] J. Gasser, M. A. Ivanov, E. Lipartia, M. Mojžiš and A. Rusetsky, *Eur. Phys. J. C* **26** (2002) 13 [arXiv:hep-ph/0206068].
- [8] T. Becher and H. Leutwyler, *Eur. Phys. J. C* **9** (1999) 643 [arXiv:hep-ph/9901384].
- [9] V. Bernard, *Prog. Part. Nucl. Phys.* **60** (2008) 82 [arXiv:0706.0312 [hep-ph]].
- [10] U.-G. Meißner, U. Raha and A. Rusetsky, *Phys. Lett. B* **639** (2006) 478 [arXiv:nucl-th/0512035].
- [11] A. M. Bernstein, *Phys. Lett. B* **442** (1998) 20 [arXiv:hep-ph/9810376].
- [12] A. M. Bernstein, M. W. Ahmed, S. Stave, Y. K. Wu and H. R. Weller, arXiv:0902.3650 [nucl-ex].
- [13] T. Becher and H. Leutwyler, *JHEP* **0106** (2001) 017 [arXiv:hep-ph/0103263].
- [14] V. Bernard, N. Kaiser and U.-G. Meißner, *Phys. Lett. B* **309** (1993) 421 [arXiv:hep-ph/9304275].
- [15] J. Gasser, V. E. Lyubovitskij, A. Rusetsky and A. Gall, *Phys. Rev. D* **64** (2001) 016008 [arXiv:hep-ph/0103157].
- [16] M. Bissegger, A. Fuhrer, J. Gasser, B. Kubis and A. Rusetsky, *Nucl. Phys. B* **806** (2009) 178 [arXiv:0807.0515 [hep-ph]].
- [17] J. Gasser and H. Leutwyler, *Phys. Rept.* **87** (1982) 77.
- [18] U.-G. Meißner, *PoS LAT2005* (2006) 009 [arXiv:hep-lat/0509029].
- [19] M. Mojžiš, *Eur. Phys. J. C* **2** (1998) 181 [arXiv:hep-ph/9704415].
- [20] P. Büttiker and U.-G. Meißner, *Nucl. Phys. A* **668** (2000) 97 [arXiv:hep-ph/9908247].
- [21] N. Fettes, U.-G. Meißner and S. Steininger, *Nucl. Phys. A* **640** (1998) 199 [arXiv:hep-ph/9803266].
- [22] N. Fettes, PhD thesis, Berichte des FZ Jülich, Jül-3814.
- [23] N. Fettes and U.-G. Meißner, *Nucl. Phys. A* **676** (2000) 311 [arXiv:hep-ph/0002162].
- [24] R. Koch and E. Pietarinen, *Nucl. Phys. A* **336** (1980) 331.
- [25] C. Haefeli, M. A. Ivanov and M. Schmid, *Eur. Phys. J. C* **53** (2008) 549 [arXiv:0710.5432 [hep-ph]].
- [26] B. Moussallam, *Nucl. Phys. B* **504** (1997) 381 [arXiv:hep-ph/9701400].
- [27] B. Ananthanarayan and B. Moussallam, *JHEP* **0406** (2004) 047 [arXiv:hep-ph/0405206].
- [28] C. Amsler *et al.* [Particle Data Group], *Phys. Lett. B* **667** (2008) 1.
- [29] M. A. Kovash [E643 Collaboration], *PiN Newslett.* **12N3** (1997) 51.
- [30] V. Bernard, N. Kaiser and U.-G. Meißner, *Phys. Lett. B* **383** (1996) 116 [arXiv:hep-ph/9603278].
- [31] V. Bernard, N. Kaiser and U.-G. Meißner, *Z. Phys. C* **70** (1996) 483 [arXiv:hep-ph/9411287].
- [32] S. R. Beane, V. Bernard, T. S. H. Lee, U.-G. Meißner and U. van Kolck, *Nucl. Phys. A* **618** (1997) 381 [arXiv:hep-ph/9702226].
- [33] J. Gasser, V. E. Lyubovitskij and A. Rusetsky, *Phys. Rept.* **456** (2008) 167 [arXiv:0711.3522 [hep-ph]].
- [34] J. Spuller *et al.*, *Phys. Lett. B* **67** (1977) 479.
- [35] M. Hoferichter, B. Kubis and U.-G. Meißner, in preparation.
- [36] W. R. Gibbs, L. Ai and W. B. Kaufmann, *Phys. Rev. Lett.* **74** (1995) 3740.
- [37] E. Matsinos, *Phys. Rev. C* **56** (1997) 3014.
- [38] J. Gasser and H. Leutwyler, *Annals Phys.* **158** (1984) 142.
- [39] J. Gasser, M. E. Sainio and A. Švarc, *Nucl. Phys. B* **307** (1988) 779.
- [40] B. Kubis and R. Lewis, *Phys. Rev. C* **74** (2006) 015204 [arXiv:nucl-th/0605006].
- [41] V. Baru, J. Haidenbauer, C. Hanhart, A. E. Kudryavtsev, V. Lensky and U.-G. Meißner, *Proc. 11th Int. Conf. on Meson-Nucleon Physics and the Structure of the Nucleon (MENU 2007), Jülich* [arXiv:0711.2743 [nucl-th]].
- [42] J. Gasser, V. E. Lyubovitskij and A. Rusetsky, arXiv:0903.0257 [hep-ph].